Short communication

Polyaniline and polypyrrole coatings on aluminum for PEM fuel cell bipolar plates

Shine Joseph [a], J.C. McClure [a], P.J. Sebastian [b,c,*], J. Moreira [c], Edgar Valenzuela [c]

[a] *Metallurgical and Materials Department, University of Texas El Paso, El Paso, TX, USA*
[b] *Centro de Investigacion en Energia, UNAM, Temixco, Morelos, Mexico*
[c] *CAES, UP Chiapas, Tuxtla Gutiérrez, Chiapas, Mexico*

Abstract

The conducting polymers polypyrrole and polyaniline were deposited on 6061 aluminum using cyclic voltammetry and painting, respectively. These samples are intended for proton exchange membrane fuel cell applications where surface contact resistance as well as bulk corrosion resistance are requirements for the bipolar plates that separate the cells. Corrosion current and voltage were measured on the samples as well as contact resistance between coated samples as a function of contact pressure. The polypyrrole samples showed neither improved corrosion resistance nor acceptable contact resistance. The painted polyaniline samples, however, showed about an order of magnitude reduction in corrosion current with only a minor increase in contact resistance. It is believed that in the more acidic environment of a fuel cell, the polyaniline will become even more conductive and that further reduction in contact resistance should be possible.
© 2007 Elsevier B.V. All rights reserved.

Keywords: Polyaniline; Polypyrrole; Aluminum; PEM fuel cell; Corrosion

1. Introduction

Proton exchange membrane (PEM) fuel cells are of interest for the transportation industry because of their low temperature operation [1–5]. Cost and portability are the major problems which restrict the commercialization of fuel cells. Size and weight are the crucial factors in mobile applications and need to be reduced as much as possible [2,4,1]. In a PEM fuel cell stack, bipolar plates contribute 80% of the size and weight and approximately 20% of the system cost. The main requirements for bipolar plates are corrosion resistance in fuel cell environment, gas impermeability, low cost, low volume, light weight, easy manufacturability, and high surface and bulk electrical conductivity.

Good bulk conductivity is required because bipolar plates separate cells in proton exchange membrane (PEM) fuel cells and carry current from cell to cell. Surface conductivity is needed because the porous carbon electrodes within the cell function both as gas diffusers and current conduction paths. These electrodes are normally pressed against the bipolar plates; hence a low resistance surface contact must be made. In addition, the plates must resist corrosion in the acidic (pH ∼3) environment of these cells [6,7].

There are many recent reports on metallic bipolar plates for PEM fuel cell application. Most of these reports are on stainless steel bipolar plates [8–15] except for a very few reports on aluminum plates [16,17]. Both stainless steel and aluminum requires protective coatings to avoid corrosion in the PEMFC environment.

The usual methods for corrosion protection produce insulating surfaces and are not applicable to PEM fuel cells. The approach adopted in this work is to use a conducting polymer coating on aluminum. In addition to low cost and weight, the aluminum can provide bulk corrosion resistance, although even slight corrosive attack can free ions that contaminate the Nafion membrane in the cell [18]. Corrosion of aluminum bipolar plates in fuel cells has been reported [2]. In addition, the surface oxide which gives aluminum corrosion resistance prevents good electrical contact between the fuel cell electrode and the aluminum bipolar plate [2,19].

---

* Corresponding author at: Centro de Investigacion en Energia, UNAM, Temixco, Morelos, Mexico. Tel.: +52 55 56229841; fax: +52 55 56229742.

E-mail address: sjp@cie.unam.mx (P.J. Sebastian).

2. Experimental details

2.1. Materials and methods

Aluminum 6061 (1.0 Mg, 0.6 Si, 0.3 Cu, 0.2 Cr) alloy was used as the substrate material in this work. Polyaniline and polypyrrole coatings were deposited on the aluminum 6061 alloy by painting and electrodeposition (cyclic voltammetry), respectively. The aluminum alloy samples were polished with 300–1200 grit SiC paper and ultrasonically cleaned in acetone and degreased in ethanol. After cleaning, the samples were covered with an acrylic resin mask leaving 1 cm^2 area exposed. The electrochemical cell for polymer deposition consisted of a platinum counter electrode, a calomel reference electrode and the prepared aluminum sample as working electrode, all connected to a 273A (EG&G) potentiostat/galvanostat. The aluminum sample was galvanostatically activated before polypyrrole electrodeposition by cyclic voltammetry. The galvanostatic activation was conducted in an electrochemical cell with platinum counter electrode, calomel reference electrode and aluminum working electrode. The electrolyte used in the galvanostatic activation was 0.1 M pyrrole dissolved in 0.1 M nitric acid and the current applied was 50 mA for 3 min. The electrolyte used in polypyrrole deposition was 0.1 M pyrrole dissolved in 0.1 M oxalic acid [20]. The polypyrrole deposition (by cyclic voltammetry) was conducted at a scan rate of 20 mV s^{-1} and the voltage scan range was −1 to 3 V vs. SCE and 3–8 cycles were used to achieve a uniform coating.

Painting was selected for developing polyaniline coatings on the Al 6061 sample. The polymer polyaniline-DNNSA (dinonylnaphthalene sulfonic acid) was provided by Crosslink Polymer Research [21]. Painting of polyaniline coating on aluminum 6061 alloy was accomplished by dissolving polyaniline in xylene, 1:1 ratio. The dissolved polymer was applied on the cleaned aluminum samples by a small brush and dried overnight. The dried samples were heated at 110 °C for 5 min to remove any air bubbles that may have trapped in the coating.

Corrosion rate studies of the coated samples were conducted in 0.1 M H$_2$SO$_4$ (pH ~3) electrolyte to simulate the fuel cell acidic environment [6]. The potentiodynamic polarization method was used for corrosion evaluation with the software "Electrochemistry Power CORR" [Princeton Applied Research]. As before, the experimental arrangement consisted of platinum counter electrode, calomel reference electrode and coated sample (1 cm^2 area exposed) as working electrode connected to a potentiostat and the scan rate was 1 mV s^{-1}.

The contact resistance of the coated samples was measured as function of compaction pressure with an ohmmeter connected between two coated aluminum samples. As mentioned above, a carbon diffuser was placed in between the coated samples during contact resistance measurement [22] to better simulate fuel cell operating conditions. All measurements were on dry rather than moist samples (which would better simulate a fuel cell environment) because of the difficulty in producing a consistent degree of water saturation.

3. Results and discussion

3.1. Galvanostatic activation of the Al 6061 sample

The voltage–time plot of the galvanostatic activation is shown in Fig. 1. The voltage applied for the surface activation of the sample was 2 V (SCE), which is slightly higher than the pitting potential of aluminum. The figure shows that the voltage 2 V vs. SCE was measured initially and then dropped to 1.9 V and stabilizes throughout the experiment. It was observed that the activation produces small pits with only very small amounts of polypyrrole. The change in surface characteristics can trigger the further polymerization and easier deposition. Several efforts were made to deposit polypyrrole on Al 6061 without pre-activation including different electrolytes, cyclic voltage ranges and potentiostatic as well as galvanostatic techniques. However, the coatings obtained from all these different electrochemical conditions other than galvanostatic pre-activation followed by cyclic voltammetry deposition were non-uniform.

3.2. Electrochemical formation of polypyrrole on Al 6061 alloy

Cyclic voltammetry was used to polymerize and deposit pyrrole on the activated Al 6061 samples. The cyclic voltammogram of the deposition process is shown in Fig. 2. As the cyclic voltage scan starts from negative to positive potentials, the current measured becomes more positive which indicates the oxidation of the monomer and aluminum. The polypyrrole formation is an oxidative polymerization and hence displacement of the cyclic scan towards the more positive current indicates the polymerization of pyrrole. In the figure, cycles 1 and 3 are shown and cycle 3 measured relatively more current than cycle 1. This indicates more oxidation and polymerization of pyrrole as the number of cycle increases. The peaks at 2 V (vs. SCE) and −0.7 V on cycle 3 represent the polymerization of pyrrole and the reduction of polypyrrole, respectively.
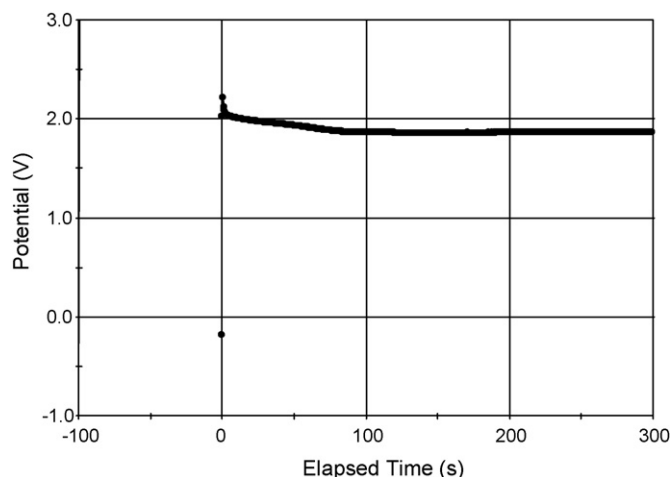

Fig. 1. Galvanostatic activation of Al 6061 sample in 0.1 M pyrrole dissolved in 0.1 M HNO$_3$ at 50 mA for 3 min.
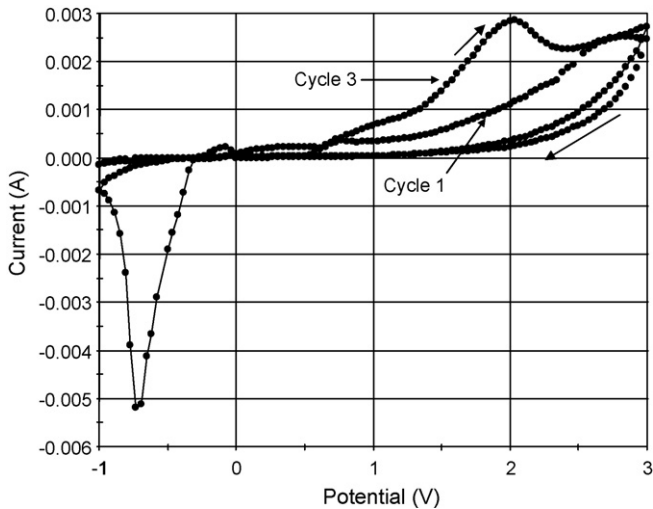
Fig. 2. The cyclic voltammogram of polypyrrole deposition on Al 6061 sample from 0.1 M pyrrole dissolved in 0.1 M oxalic acid. Cycles 1 and 3 are shown in the figure.

3.3. Infrared spectroscopy

Fig. 3 shows the FTIR spectra of polypyrrole deposited on Al 6061 from 0.1 M pyrrole dissolved in 0.1 M oxalic acid. Peaks at 580 and 480 cm^{-1} are N–H wag and C=C out of plane bend vibrations, respectively. The peak between 1000 and 1100 cm^{-1} represents C–N bond vibrations and peaks 1040, 960 cm^{-1} are showing the ring vibrations of pyrrole [20,23].

3.4. Corrosion rate of polypyrrole coated (electrodeposited) Al 6061 sample

Fig. 4 shows a comparison of the corrosion resistance of polypyrrole coated Al 6061 sample with an uncoated aluminum sample. Corrosion current density of the coated sample is supposed to be lower than the uncoated sample. But the results show that both coated and uncoated samples have the same corrosion current density ($\sim 10^{-5}$ A cm^{-2}). In fact, in some corrosion tests the polypyrrole coated samples showed higher corrosion current than the uncoated plates. This indicates that the polypyrrole coating assists in the aluminum oxidation
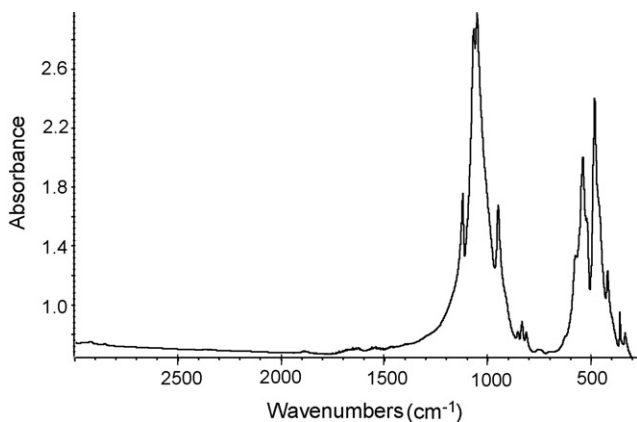

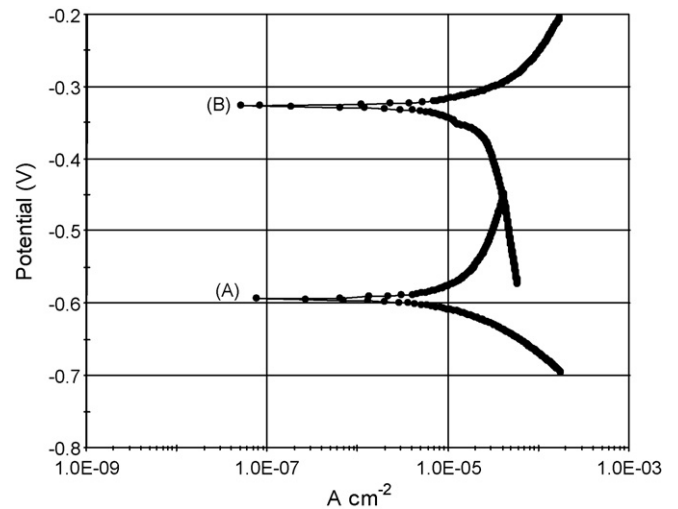Fig. 3. The FTIR spectra of electrodeposited polypyrrole on Al 6061.

Fig. 4. The potentiodynamic polarization curves of polypyrrole coated (electrodeposited) Al 6061 compared with the uncoated sample. (A) Uncoated Al 6061 sample, (B) polypyrrole coated Al 6061 sample.

process as an oxidizing agent which enhances the corrosion process.

However, the corrosion potential of the coated sample shifts towards a more positive value with respect to the uncoated sample (Fig. 4). This indicates the presence of aluminum oxide forming underneath the coating during deposition. The relatively high contact resistance (discussed in Section 3.6 below) of the coated sample again indicates the same conclusion.

Fig. 5A shows the optical micrographs of galvanostatically activated Al 6061 sample. The activated sample has numerous pits filled with polypyrrole. A polypyrrole deposited sample is shown in Fig. 5B. The polypyrrole coating formed on Al 6061 has pin-holes throughout the coating. The frequent pin holes seen in Fig. 5C explain the poor corrosion performance seen in Fig. 4. It was also observed that the pits are not completely covered with polypyrrole which leads to further corrosion of the substrate.

In the case of polypyrrole coatings on Al 6061, it was observed that 3–8 cycles were appropriate for good coatings but above 10 cycles the substrate starts to corrode aggressively as seen in Fig. 5D by the large pits formed on the polypyrrole deposited Al 6061 with 20 cycles. Polypyrrole deposition parameters used in this work were acidic electrolyte and voltage ranges of −1 to 3 V (vs. SCE). It was known that these conditions were likely to cause corrosion in the aluminum alloy, but they were necessary for the uniform polypyrrole coating on Al 6061 substrate.

3.5. Corrosion results of polyaniline painted Al 6061 samples

The change in corrosion resistance with polyaniline coating thickness on Al 6061 is shown in Fig. 6. Both the 40 and the 5 μm thick coatings showed reduction in corrosion current of 10^{-3} and 10^{-1}, respectively, compared to uncoated aluminum plate. As expected, the corrosion resistance of the 40 μm thick
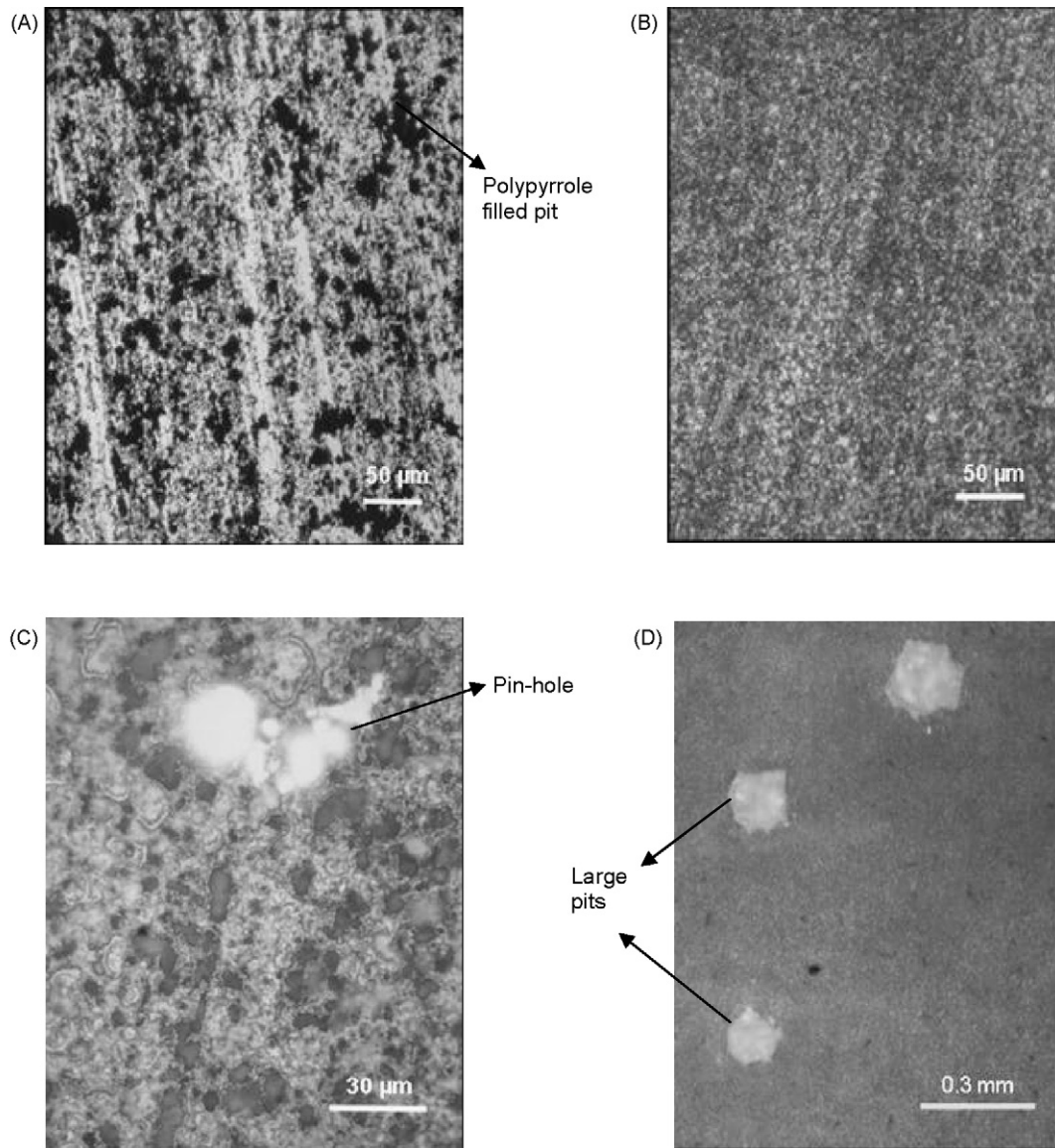
Fig. 5. The optical micrographs of polypyrrole coated Al 6061 samples. 5(A) Galvanostatically activated sample, 5(B) polypyrrole coated (5 Cycles) Al 6061 sample, 5(C) pin-holes observed on the polypyrrole coated sample at high magnification, 5(D) polypyrrole coating deposited in 20 cycles.
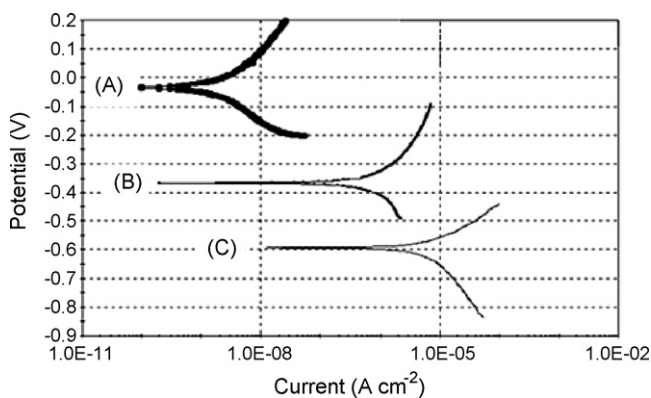

Fig. 6. Variation in corrosion resistance with coating thickness. (A) Polyaniline painted Al 6061 with coating thickness $\sim$40 μm, (B) Al 6061 with polyaniline coating thickness $\sim$5 μm, (C) uncoated Al 6061 plate.

polyaniline coated plate (10^{-8} A cm^{-2}) is better than the 5 μm thick coating (10^{-6} A cm^{-2}) due either to pinholes or diffusion of oxidizing agents through the thin coating.

3.6. Contact resistance of polyaniline and polypyrrole coated Al 6061 samples

Contact resistance measurements of polypyrrole were conducted in a dry rather than a moist simulated fuel cell condition. The contact resistance was measured as a function of compaction pressure as shown in Fig. 7. For comparison, uncoated plates with and without a diffuser were measured.

The contact resistance of polypyrrole coated samples showed a contact resistance of approximately 1 Ω cm^2 at 250 N cm^{-2} compaction pressure. Therefore, using these coated plates in fuel cells may affect the cell performance. Above 200 N cm^{-2} compaction pressure, the electrical resistance stabilizes around
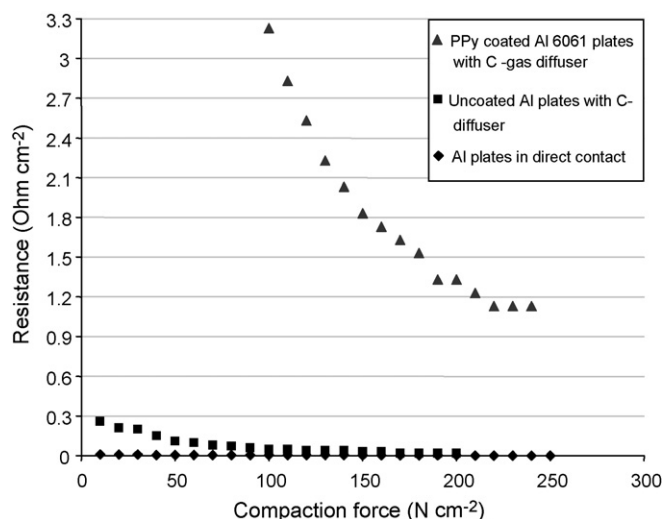
Fig. 7. The contact resistance of polypyrrole coated (electrodeposited) Al 6061 plates compared with the uncoated Al plates in simulated fuel cell condition.

$1 \, \Omega \, cm^2$. The higher contact resistance shown in the graph indicates that a non-conductive aluminum oxide layer formed underneath the coating during deposition.

In Fig. 8 contact resistance of polyaniline painted Al 6061 samples ($\sim 5 \, \mu m$ thick coatings) compared with the uncoated and graphite plates are shown. The contact resistance of the uncoated plates, coated plates, uncoated–coated plates and graphite plate combinations were compared in Fig. 8. The uncoated aluminum plates with carbon diffuser show the least resistance and the polymer coated plates with carbon diffuser shows the highest ($0.3 \, \Omega \, cm^2$). It is seen that the contact resistance stabilizes above $150 \, N \, cm^{-2}$ compaction pressure and that the more the interfaces between the aluminum substrates, the higher the resistance. No data is shown for the 40 μm polyaniline coating because it had a very high contact resistance.

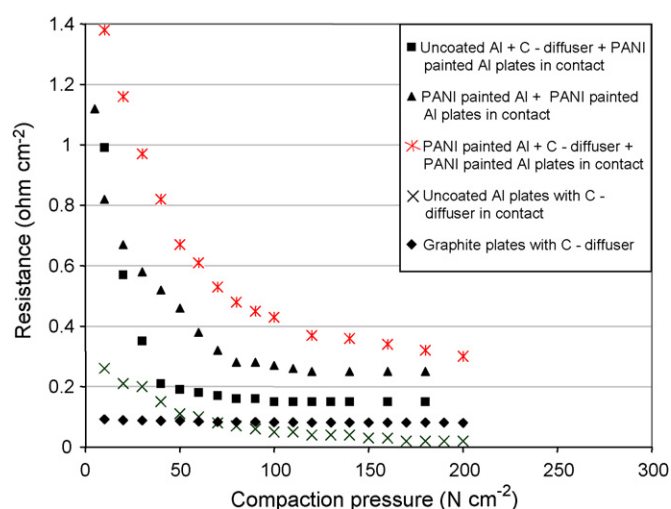The conductivity of both polymers is related to their degree of oxidation or reduction by a dopant [24]. Therefore, these polymers should be more conductive in the acid environment of a fuel cell. Although a target for contact resistance is less than $0.1 \, ohm \, cm^2$, the observed dry air contact resistance of the polyaniline coated plates (0.2–$0.3 \, \Omega \, cm^2$) is expected to be satisfactory for actual fuel cell application.

4. Conclusions

Polypyrrole coatings were deposited electrochemically on 6061 Al. The corrosion resistance of the polypyrrole coated samples showed no significant improvement from the uncoated plates, and the contact resistance was higher than uncoated plates. The polyaniline painted Al 6061 plates showed very good corrosion resistance compared to the uncoated aluminum plates while exhibiting only slightly higher contact resistance than the standard graphite plates. These polymers are more conductive in acidic (oxidizing) environment because conductivity of these polymers is directly related to their degree of oxidation. Since the conductivity of polyaniline increases with its degree of oxidation, it is possible that in the acid environment of a fuel cell, the resistance will be even lower than what is reported in this article.

References

[1] I. Bar-On, R. Kirchain, R. Roth, J. Power Sources 109 (2002) 71–75.
[2] A.S. Woodman, E.B. Anderson, K.D. Jayne, M.C. Kimble, Proceedings of the AESF SUR/FIN '99 6 (1999) 21–24.
[3] J. Wind, R. Spah, W. Kaiser, G. Bohm, J. Power Sources 105 (2002) 256–260.
[4] H. Tsuchiyaa, O. Kobayashi, Int. J. Hydrogen Energy 29 (2004) 985–990.
[5] B. James, F. Lomax, S. Thomas, W. Colella, PEM Fuel Cell Power System Cost Estimates: Sulfur-Free Gasoline Partial Oxidation and Compressed Direct Hydrogen, report for the U.S. Department of Energy, 1997.
[6] Y. Li, Troy, et al., US Patent 5,624,769 (1997).
[7] S.-J. Lee, C.-H. Huang, J.-J. Lai, Y.-P. Chen, J. Power Sources 131 (2004) 162–168.
[8] R.C. Makkus, A.H.H. Janssen, F.A. de Bruijn, R.K.A.M. Mallant, J. Power Sources 86 (2000) 274–282.
[9] H. Wang, M.A. Sweikart, J.A. Turner, J. Power Sources 115 (2003) 243–251.
[10] J.S. Cooper, J. Power Sources 129 (2004) 152–169.
[11] H. Wang, M.P. Brady, G. Teeter, J.A. Turner, J. Power Sources 138 (2004) 86–93.
[12] H. Wang, M.P. Brady, K.L. More, H.M. Meyer JrIII, J.A. Turner, J. Power Sources 138 (2004) 79–85.
[13] E.A. Cho, U.-S. Jeon, S.-A. Hong, I.-H. Oh, S.-G. Kang, J. Power Sources 142 (2005) 177–183.
[14] H. Wang, J.A. Turner, J. Power Sources 170 (2007) 387–394.
[15] Y.W. Derek, O. Northwood, J. Power Sources 165 (2007) 293–298.
[16] Y. Hung, K.M. El-Khatib, H. Tawfik, J. Power Sources 163 (2006) 509–513.
[17] C. Shen, M. Pan, Z. Hua, R. Yuan, J. Power Sources 166 (2007) 419–423.

Fig. 8. The contact resistance of polyaniline painted ($\sim 5 \, \mu m$ thickness), uncoated and graphite plates compared in simulated fuel cell condition.

[18] R.C. Makkus, A.H.H. Janssen, F.A. de Bruijin, K.A.M.M. Ronald, J. Power Sources 86 (2000) 274–282.

[19] D.E. Tallman, et al., Curr. Appl. Phys. 4 (2004) 137–140.

[20] G.S. Akundi, R. Rajagopalan, J.O. Iroh, J. Appl. Polym. Sci. 83 (2002) 1970–1977.

[21] Crosslink Polymer Research, 950 Bolger Court Fenton, MO 63026-2029.

[22] S. Joseph, J.C. McClure, R. Chianelli, P. Pich, P.J. Sebastian, Int. J. Hydrogen Energy 30 (2005) 1339–1344.

[23] K. Shah, Y. Zhu, J.O. Iroh, O. Popoola, Surf. Eng. 17 (2001) 405–412.

[24] D. Kumar, R.C. Sharma, Eur. Polym. J. 34 (1998) 1053–1060.